

CARE What Fails: Contrastive Anchored-REflection for Verifiable Multimodal Reasoning

Yongxin Wang¹, Zhicheng Yang², Meng Cao¹, Mingfei Han¹, Haokun Lin¹, Yingying Zhu³, Xiaojun Chang¹, Xiaodan Liang¹

¹ Mohamed bin Zayed University of Artificial Intelligence

² The Hong Kong University of Science and Technology (Guangzhou) ³ Transsion

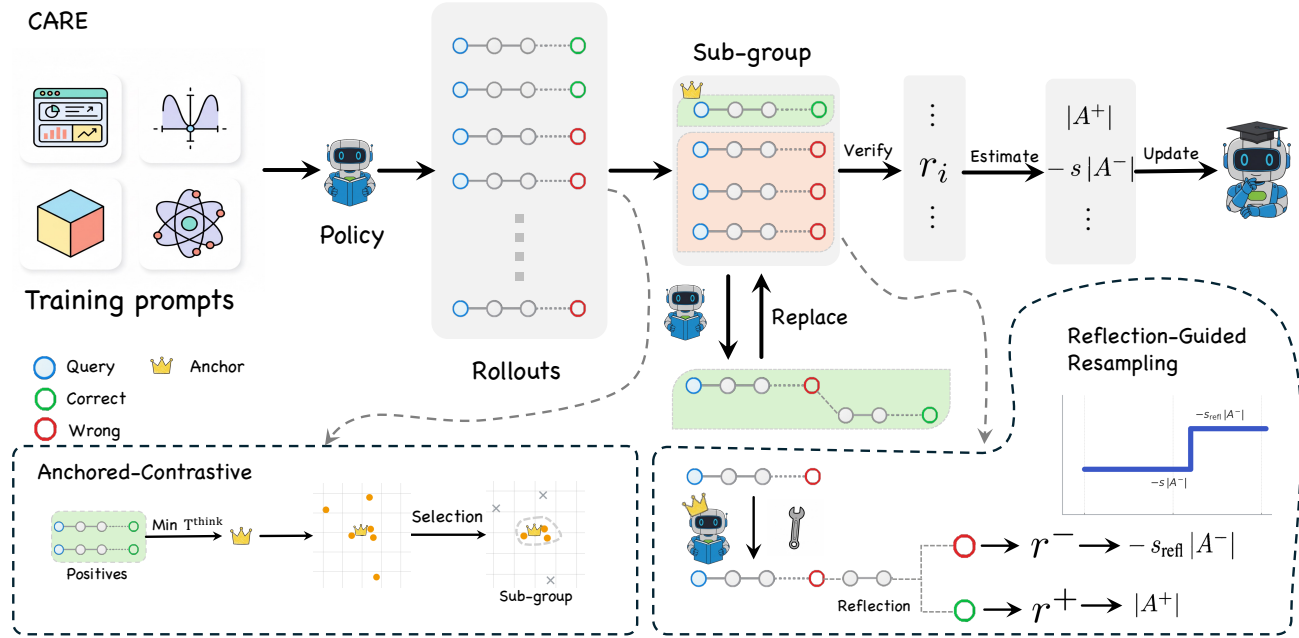


Figure 1. **Overview of CARE.** Given a multimodal prompt, the policy samples a fixed number of rollouts. A programmatic verifier scores the answer with rationale and supplies the reward used to update the policy. *Anchored-contrastive* (bottom-left): pick the anchor as the verified-correct rollout with the shortest rationale; form a subgroup by selecting hard negatives that fail the verifier but are closest in rationale to the anchor. Advantages are normalized within this subgroup, and negatives are down-weighted. *Reflection-Guided Resampling* (bottom-right): pair exactly one positive with one hard negative, insert a brief repair cue, and resample the negative once—on success replace the failure; otherwise keep it with a reduced penalty.

Abstract

Group-relative reinforcement learning with verifiable rewards (RLVR) often wastes the most informative data it already has—the failures. When all rollouts are wrong, gradients stall; when one happens to be correct, the update usually ignores why the others are close-but-wrong, and credit can be misassigned to spurious chains. We present **CARE** (Contrastive Anchored REflection), a failure-centric post-training framework for multimodal reasoning that turns errors into supervision. CARE combines: (i) an anchored-

contrastive objective that forms a compact subgroup around the best rollout and a set of semantically proximate hard negatives, performs within-subgroup z-score normalization with negative-only scaling, and includes an all-negative rescue to prevent zero-signal batches; and (ii) Reflection-Guided Resampling (RGR), a one-shot structured self-repair that rewrites a representative failure and re-scores it with the same verifier, converting near-misses into usable positives without any test-time reflection. CARE improves accuracy and training smoothness while explicitly increasing the share of learning signal that comes from failures. On

Qwen2.5-VL-7B, CARE lifts macro-averaged accuracy by 4.6 points over GRPO across six verifiable visual-reasoning benchmarks; with Qwen3-VL-8B it reaches competitive or state-of-the-art results on MathVista and MMMU-Pro under an identical evaluation protocol.

1. Introduction

Large Language Models (LLMs) have advanced text comprehension, generation, and reasoning, catalyzing the development of Large Multimodal Models (MLLMs) that integrate vision and language. Early MLLMs (e.g., GPT-4V [27], LLaVA [18]) demonstrate strong abilities in captioning and conversational visual-question answering (VQA), but the frontier has shifted toward complex, compositional reasoning in domains such as mathematics, science, and engineering. Recent benchmarks MathVista [23], MathVerse [49], MATH-Vision [38], and MMMU [25] reveal persistent gaps: while strong systems can exceed 70–80% on *MathVista*, errors concentrate on visually grounded, compositional reasoning, underscoring that outcome-only supervision still provides weak guidance for long-horizon reasoning.

Reinforcement Learning with Verifiable Rewards (RLVR) offers a promising alternative by using programmatic verifiers (e.g., answer checkers) to provide deterministic, scalable rewards [7, 26]. Group-based methods such as Group Relative Policy Optimization (GRPO) [33] make RLVR practical by comparing multiple rollouts per query [33]. However, two limitations remain salient under small rollout budgets: (1) high gradient variance and training instability, (2) flawed credit assignment, which can reinforce spurious chains of reasoning when a correct answer is reached by chance.

We introduce **CARE** (*Contrastive Anchored REflection*), a verifier-driven post-training framework that is explicitly failure-centric. CARE turns informative errors into learning signal in two complementary ways. First, an *anchored-contrastive objective* treats the best rollout as an anchor and normalizes rewards *within* a curated subgroup of hard negatives, yielding a stable, scale-aware contrast that teaches the policy to separate correct solutions from plausible failures while assigning credit in a fail-aware manner. Second, a lightweight *Reflection-Guided Resampling* step performs a one-shot, error-corrective resample on a selected hard negative whenever a group contains a successful rollout, so representative mistakes are actively converted into improvements rather than passively ignored.

We validate on MathVista, MathVerse, MATH-Vision, and MMMU-Pro. Under identical inference-time budgets, CARE achieves state-of-the-art performance on MathVista and MMMU-Pro, and consistently surpasses strong RLVR baselines such as GRPO [33], DAPO [44] and GSPO [50]

on all benchmarks, indicating a stable and effective path to training reliable multimodal reasoners.

Contributions. Our contributions are threefold:

- **Anchored-contrastive objective.** We anchor advantages to the best rollout and normalize *within* a subgroup of hard negatives, producing a stable, contrastive, and scale-aware learning signal with improved, fail-aware credit assignment.
- **Reflection-Guided Resampling.** We introduce a single-shot guided resample on a selected hard negative in success-containing groups, turning representative failures into improvements rather than discarding them.
- **Empirical gains on visual reasoning.** CARE sets new SOTA on MathVista and MMMU-Pro and delivers consistent improvements on MathVerse and MATH-Vision over established RLVR baselines.

2. Related Works

Reinforcement Learning with Verifiable Reward
RLVR fine-tunes LLMs using objective, easily checked rewards (e.g., pass/fail) instead of preference models, and has delivered large gains on math and coding [7, 26, 33]. A key enabler is Group Relative Policy Optimization (GRPO) [33], a PPO-style method that replaces a learned value critic with group-based Monte Carlo advantages; GRPO underpinned DeepSeek-R1’s binary-reward training. Critic-free baselines such as RLOO [1] and sequence-level variants like GSPO [50] broaden the design space. To address long-horizon reasoning and stability, recent work refines GRPO: Dr.GRPO [20] removes a length-inflation bias to improve token efficiency without hurting accuracy; DAPO [44] adds asymmetric clipping and selective rollouts for stability and sample efficiency; and DARS [31] targets hard prompts with difficulty-adaptive multi-stage rollouts, improving long-tail Pass@K at no extra inference cost.

Multimodal Large Reasoning Models
Recent efforts show that reinforcement learning (RL) fine-tuning substantially strengthens multimodal large language models (MLLMs) when paired with curated chain-of-thought (CoT) data and stabilizing training strategies. Bootstrapped pipelines such as MMR1 [14] and Vision-R1 [12] report consistent gains on math-with-images benchmarks. Moving beyond outcome-only rewards, process-aware methods explicitly incentivize better reasoning chains: SophiaVL-R1 [8] trains a “thinking” reward model with Trust-GRPO; VL-Rethinker [37] forces a self-verification “rethinking” step with selective replay; ARES [6] adapts reasoning length via entropy-shaped exploration; and VPPO [41] reweights policy updates toward visually grounded tokens. RL has also been used to endow LVLMs with task-specific skills through explicit reasoning modules and composite rewards—e.g., MetaSpatial [15] visual reasoning, ViGoRL [32] for spatially grounded exploration, GUI-R1 [21] for

GUI agents, and R1-Track [48] for long-horizon tracking. Robustness and stability are improved by visual perturbation during rollouts or fine-tuning [17, 19] and by sampling schemes that maintain reward variance [14]. To mitigate data scarcity, two-stage pipelines leverage cold-start SFT then RL on curated reasoning corpora (e.g., Vision-R1-cold [12]; MMR1-SFT [14]). Finally, tool- and domain-aware RL extends reasoning to specialized settings, including visual tool use [16], clinically faithful radiology reports [39], and long-horizon video reasoning with sequence-parallel RL [34].

Multimodal Reasoning Prior work on multimodal reasoning commonly evaluates on visual-math or physical benchmarks such as MathVista [23], MathVerse [49], MATH-Vision[38], and SeePhys [11] which probe diagram comprehension and stepwise quantitative reasoning while providing objective answer formats (e.g., exact-match or multiple-choice) that align naturally with verifiable rewards. Beyond mathematics, MMMU-Pro [45] extends assessment to college-level, multi-disciplinary problems across heterogeneous visual modalities, mitigating textual shortcuts and strengthening measurement of genuine visual grounding under RLVR ; we also reference the broader MMMU suite [25]. Recently, reasoning-centric corpora such as ViRL39K[35], LLaVA-CoT[30], M3CoT[5], MMK12[9], and R1-OneVision[43] emphasize deliberate reasoning with objectively gradable end answers—making them natural fits for RLVR training and evaluation.

3. Methodology

Overview. We optimize under *verifiable* rewards while keeping test-time decoding unchanged (*single decode, no reflection*). CARE combines an anchored-contrastive objective with a *training-only* reflection step when a success exists. (1) An *anchored-contrastive objective* anchors sequence-level advantages to the best rollout and normalizes them within a hard-negative subgroup, with negative-penalty scaling and an all-negative rescue. (2) *Reflection-Guided Resampling* (RGR) augments training by selecting one hard negative, inserting a brief repair cue into its rationale, and resampling exactly one reflected response. The policy is then updated on the augmented group; reflected successes replace the original failure, and reflected failures receive a reduced penalty. An overview is shown in Fig. 1.

3.1. Problem Setting and Notation

We study verifiable multimodal reasoning over inputs $x = (\mathbf{I}, \mathbf{q})$, where \mathbf{I} denotes one or more images and \mathbf{q} denotes a text query. The policy $\pi_\theta[y \mid x]$ emits $\langle \text{think} \rangle \hat{r} \langle / \text{think} \rangle$ followed by $\langle \text{answer} \rangle \hat{y} \langle / \text{answer} \rangle$. A programmatic verifier \mathcal{V} parses only the answer span and returns two bounded signals $\text{acc}[x, y] \in [0, 1]$ and $\text{fmt}[x, y] \in [0, 1]$. We define the

overall reward

$$r_i = [1 - \lambda] \cdot \text{acc}[x, y_i] + \lambda \cdot \text{fmt}[x, y_i], \quad \lambda \in [0, 1]. \quad (1)$$

For each prompt we draw G rollouts $\mathcal{Y} = \{y_1, \dots, y_G\}$ with rewards $r_i = r[y_i]$. Let T_i be the total number of response tokens, T_i^{ans} those inside $\langle \text{answer} \rangle \dots \langle / \text{answer} \rangle$, and T_i^{think} those inside $\langle \text{think} \rangle \dots \langle / \text{think} \rangle$. We denote by π_{old} the frozen sampling policy for the current batch, and by π_{ref} a fixed reference policy used only for KL regularization.

3.2. CARE: Anchored-Contrastive Subgroup

Anchor. Let $\mathcal{P} = \{i : \text{acc}[x, y_i] = 1\}$ be the positive set under the verifier. If $\mathcal{P} \neq \emptyset$, choose the anchor

$$y^+ = \arg \min_{i \in \mathcal{P}} T_i^{\text{think}}, \quad (2)$$

breaking ties toward shorter answers T_i^{ans} . If $\mathcal{P} = \emptyset$, anchoring is bypassed and the group is handled by the all-negative rescue in Sec. 3.7.

Hard negatives. Let \mathcal{N} be the hard negatives returned by the selector in Sec. 3.3. When the number of negatives is fewer than the target subgroup size K , we shrink to fit:

$$\begin{aligned} K' &= \min(K, |\{i : \text{acc}[x, y_i] = 0\}|), \\ S &= \{y^+\} \cup \{y_1^-, \dots, y_{K'}^-\}. \end{aligned} \quad (3)$$

If $K' = 0$, we skip the update to avoid arbitrary drift under saturated rewards.

3.3. Negative Selection

We seek negatives that are *close in rationale* yet wrong in outcome, so the contrast focuses on near misses rather than heterogeneous error types. We therefore use verifier correctness only as a binary gate and rank failures by cosine proximity to the anchor. Let the failure pool be $\mathcal{F} = \{i : \text{acc}[x, y_i] = 0\}$. For each $i \in \mathcal{F}$, form a rationale embedding by mean-pooling final-layer hidden states over the $\langle \text{think} \rangle$ span and ℓ_2 -normalizing; denote the anchor’s embedding by \tilde{h}_+ . We do *not* backpropagate through these embeddings (stop-gradient).

$$d_{\text{cos}}(i) = 1 - \tilde{h}_i^\top \tilde{h}_+. \quad (4)$$

We rank \mathcal{F} by ascending d_{cos} and take the top K' items as hard negatives. To curb redundancy, we first preselect the top $M > K'$ nearest and apply a brief farthest-first pass within this subset before returning the final K' ; hyperparameter details for M are provided in the Appendix. The selected set supplies the subgroup S used by the within-group normalization in Eqs. (5)–(7) and the negative considered for reflection in Sec. 3.6.

3.4. Group-Normalized Advantages

Within-group normalization. Given the current subgroup S , define

$$\mu_S = \frac{1}{|S|} \sum_{y \in S} r[y], \quad (5)$$

$$\sigma_S = \sqrt{\frac{1}{|S|} \sum_{y \in S} (r[y] - \mu_S)^2} + \varepsilon. \quad (6)$$

We first form *raw* (pre-scaling) sequence-level advantages

$$A_{\text{raw}}[y] = \begin{cases} \frac{r[y] - \mu_S}{\sigma_S}, & y \in S, \\ 0, & y \notin S. \end{cases} \quad (7)$$

A robust variant replaces μ_S by a trimmed mean and σ_S by a median absolute deviation with the same ε .

Negative-penalty scaling and update-size equalization. To mitigate over-sharpening we down-weight only negatives and leave the anchor unchanged:

$$\begin{aligned} \forall y_j^- \in S : \quad A[y_j^-] &\leftarrow -s |A_{\text{raw}}[y_j^-]|, \\ A[y^+] &\leftarrow A_{\text{raw}}[y^+]. \end{aligned} \quad (8)$$

with $s \in (0, 1]$. When $K' < K$, a global rescale $A \leftarrow \sqrt{K/K'} A$ equalizes update magnitude across groups of different K' without changing direction.

Mechanistic signature. Assume a near two-level pattern inside S with one anchor at r^+ and negatives around m_- , and let $\Delta = r^+ - m_- > 0$. z-score normalization yields

$$A_{\text{raw}}[y^+] \approx \alpha \sqrt{K'}, \quad \bar{A}_{\text{raw}}[y_j^-] \approx -\alpha \frac{1}{\sqrt{K'}}, \quad (9)$$

with attenuation $\alpha = (1 + \frac{(K'+1) \text{Var}_-}{\Delta^2})^{-1/2} \in (0, 1]$. For strictly binary rewards and $\Delta = 1$ this reduces to

$$A_{\text{raw}}[y^+] = \sqrt{K'}, \quad A_{\text{raw}}[y_j^-] = -\frac{1}{\sqrt{K'}}. \quad (10)$$

Note. The *final* advantages used by the optimizer are obtained from A_{raw} by applying negative-penalty scaling s (negatives only) and, when $K' < K$, the global equalization factor $\sqrt{K/K'}$. The proof is shown in Appendix Sec. 7.

3.5. Token-Weighted Policy Objective

Let $\rho_{i,t} = \exp(\log \pi_\theta[y_{i,t} | x] - \log \pi_{\text{old}}[y_{i,t} | x])$. Define region weights $w_{i,t}$ as follows: tokens inside the answer span receive weight 1; tokens inside the rationale span

receive weight γ^+ if i is a positive sample and 0 if i is a negative sample. Normalize per-token advantages

$$a_{i,t} = A[y_i] \cdot \frac{w_{i,t}}{\sum_{u=1}^{T_i} w_{i,u} + \epsilon_w}. \quad (11)$$

We use $\gamma^+ = 0.005$ in all main results, and set $\epsilon_w, \varepsilon > 0$ as small constants for numerical stability. The clipped surrogate is

$$\mathcal{L}_{\text{PG}} = - \frac{1}{|S^*|} \sum_{i \in S^*} \sum_{t=1}^{T_i} \min \left\{ \rho_{i,t} a_{i,t}, \right. \\ \left. \text{clip}(\rho_{i,t}, 1 - \epsilon_{\text{low}}, 1 + \epsilon_{\text{high}}) a_{i,t} \right\}, \quad (12)$$

where $S^* = \{i : A[y_i] \neq 0\}$. We add a regularizer

$$\mathcal{L} = \mathcal{L}_{\text{PG}} + \beta \text{KL}[\pi_\theta \| \pi_{\text{ref}}]. \quad (13)$$

3.6. Reflection-Guided Resampling

RGR augments the anchored-contrastive training when a verifier-positive anchor exists. Select exactly one positive y^+ and one hard negative y^- according to Sec. 3.3. Insert a brief repair cue inside the rationale span and resample:

```
<think>
Your previous reasoning was
incorrect. Identify the failing
operation, correct it, and re-derive
the necessary quantities.
Keep this section concise. Do not
restate the question.
</think>
<answer> FINAL_ANSWER_HERE </answer>
```

Decode exactly one additional rollout for y^- with the same decoding hyperparameters and rescore it with the same verifier. Run the anchored-contrastive update on the augmented group and apply two safeguards: if the reflected sample succeeds, replace the original failed rollout from the subgroup; if it fails, keep it as a negative and use a reduced negative-penalty scaling for that item (use Eq. (8) with a smaller factor $s_{\text{refl}} \in (0, s]$). RGR is disabled in all-negative groups. *Default settings.* We set $s=0.5$ and $s_{\text{refl}}=s/2$ across all main results.

3.7. All-Negative Rescue with Partial Balance

If $\max_i r_i$ is near zero, the group-relative gradient nearly vanishes. We inject a small zero-sum pseudo-contrast on a subset $S = \{t\} \cup \mathcal{N}$ where t is a pseudo-anchor (chosen as the failure with the highest $\log \pi_{\text{old}}(y | x)$) and \mathcal{N} contains $K' = \min(K, |\mathcal{F}|)$ representative negatives. On S only, assign

$$\begin{aligned} r'[t] &= \delta, \\ r'[j] &= -\frac{\delta}{K'} \quad \text{for } j \in \mathcal{N}, \\ r'[u] &= 0 \quad \text{for } u \notin S. \end{aligned} \quad (14)$$

Table 1. Evaluation of vision–language models on multimodal reasoning benchmarks. The best and second-best in each column are marked in **bold** and underlined, respectively. A dash (—) indicates a result was not reported.

Models	MathVista _{mini} [23]	MathVerse _{mini} [49]	MATH-Vision _{full} [38]	MMMU _{val} [25]	MMMU-Pro _{standard} [45]	MMMU-Pro _{vision} [45]
<i>Proprietary Models</i>						
GPT-4o [28]	63.8	37.6	—	—	—	—
GPT-5-Nano [29]	73.1	—	59.7	72.6	—	—
Claude-Sonnet-3.7 [3]	66.8	—	41.9	75.0	—	—
Gemini-2.0-Pro [10]	71.3	67.3	48.1	69.9	—	—
<i>Instruct Models</i>						
Qwen2.5-VL-3B [4]	62.0	47.6	21.2	46.4	31.1	21.3
Qwen2.5-VL-7B [4]	68.6	49.2	22.4	61.3	36.3	32.8
Qwen3-VL-4B-Instruct [42]	73.7	46.8	51.6	67.4	—	—
Qwen3-VL-8B-Instruct [42]	77.2	62.1	53.9	69.6	—	—
InternVL3.5-8B-Instruct [40]	74.2	—	46.4	68.1	—	—
MiMo-VL-7B-SFT [46]	<u>81.8</u>	67.1	57.9	64.6	45.2	39.4
LLaVA-OneVision-1.5 8B [2]	69.6	—	25.6	55.4	37.4	25.2
<i>Reasoning Models</i>						
DeepEyes [51]	70.1	47.3	26.6	—	—	—
M2-Reasoning [36]	75.0	—	31.5	—	—	—
Qwen3-VL-4B-Thinking [42]	79.5	<u>75.2</u>	60.0	70.8	—	—
Qwen3-VL-8B-Thinking [42]	81.4	<u>77.7</u>	62.7	<u>74.1</u>	—	—
MiMo-VL-7B-RL [46]	81.5	71.5	60.4	66.7	<u>46.2</u>	<u>40.3</u>
Vision-R1-7B [12]	73.5	—	—	—	—	—
Keye-VL-1.5-8B [13]	80.7	59.8	46.0	71.4	—	—
InternVL3.5-8B-MPO [40]	74.2	—	46.4	71.2	—	—
<i>RLVR Baselines</i>						
Qwen2.5-VL-7B + GRPO [33]	68.9	50.8	25.7	61.1	36.4	32.8
Qwen2.5-VL-7B + DAPO [44]	72.6	54.2	29.4	61.6	37.3	34.7
Qwen2.5-VL-7B + GSPO [50]	74.1	56.0	31.6	62.2	38.9	36.4
<i>Our Models</i>						
Qwen2.5-VL-3B + CARE	66.5	49.9	25.0	47.2	33.1	24.0
Qwen2.5-VL-7B + CARE	74.7	56.8	32.6	62.5	39.7	37.1
Qwen3-VL-8B-Instruct + CARE	82.1	69.7	<u>61.7</u>	71.0	46.7	41.7

Then compute Eq. (7) on S using r' , apply Eq. (8) to negatives, and proceed with Eqs. (11) to (13). This reproduces Eq. (10) and yields a well-conditioned update without modifying the true reward. *Default magnitude*. We fix the pseudo-contrast to $\delta=0.1$ for all main experiments.

4. Experiments

4.1. Experimental Setup

Training protocol. We construct a visual reasoning training set by combining ChartQA [24], Geometry3K [22], and ViRL39K [37]; after deduplication and format normalization this yields about 49.3K unique multimodal prompts. Dataset details are shown in Section 8.1. Each training sample consists of an image (e.g., a chart or diagram) paired with a question; the model must produce a step-by-step rationale in `<think>` followed by a final answer in `<answer>`. Before RL post-training, we perform a cold-start supervised fine-tuning on the Vision-R1-cold [12] dataset to bootstrap format adherence and basic visual-math reasoning. Our method uses an *anchored-contrastive objective* with an anchor-aware hard-negative subgroup of size $K=4$, z-score normalization within the subgroup, and negative-penalty scaling; when all rollouts are negative, a small zero-sum pseudo-contrast is injected to avoid stalls (Section 3.7). *Reflection-Guided Resampling* is *positive-paired*: it triggers only when a group contains at

least one successful rollout, and performs a single guided resample on a selected hard negative during training without increasing the inference-time budget. Unless otherwise noted, we run **five** independent random seeds ($n=5$) and report the *mean*; the corresponding 95% confidence intervals (CIs) are provided in the Appendix.

Evaluation protocol. We use MathVista, MathVerse, MATH-Vision, MMMU_{val}, MMMU-Pro_{standard}, and MMMU-Pro_{vision}, all of which provide programmatically verifiable answer keys for exact-match evaluation on the `<answer>` span. All evaluations are conducted with the official LMMs-Eval [47]. All methods use a *single decode per example* under identical decoding hyperparameters; no reflection is used at inference time.

Models and Baselines. Our backbones are Qwen2.5-VL-3B, Qwen2.5-VL-7B, and Qwen3-VL-8B-Instruct. On each backbone we report the Instruct model and our CARE model. For RLVR baselines we include GRPO [33], DAPO [44], and GSPO [50], trained on the same 49.3K mixture with the same rollout budget $G=8$, identical decoding, and a matched optimization budget (Appendix Section 8.2).

4.2. Main Results

Table 1 reports accuracy on six verifiable visual–reasoning benchmarks. On MathVista_{mini} our best model Qwen3-VL-8B + CARE reaches **82.1**, surpassing all

Table 2. Ablation on the two components of CARE. Anchor = anchored-contrastive objective; RGR = reflection-guided resampling. Avg. is the macro average over the six benchmarks; Δ is the macro gain over GRPO on the same backbone.

Model Config.	Components		MathVista _{mini}	MathVerse _{mini}	MATH-Vision _{full}	MMMU _{val}	MMMU-Pro _{std}	MMMU-Pro _{vision}	Avg.	Δ vs GRPO
	Anchor	RGR								
Backbone: Qwen2.5-VL-3B										
Base (Instruct)	\times	\times	62.0	47.6	21.2	46.4	31.1	21.3	38.27	-0.56
GRPO (Baseline)	\times	\times	63.5	47.9	22.4	45.4	31.9	21.9	38.83	—
CARE w/o RGR	\checkmark	\times	65.3	48.2	24.7	47.4	32.2	23.1	40.15	+1.32
CARE	\checkmark	\checkmark	66.5	49.9	25.0	47.2	33.1	24.0	40.95	+2.12
Backbone: Qwen2.5-VL-7B										
Base (Instruct)	\times	\times	68.6	49.2	22.4	61.3	36.3	32.8	45.10	-0.85
GRPO (Baseline)	\times	\times	68.9	50.8	25.7	61.1	36.4	32.8	45.95	—
CARE w/o RGR	\checkmark	\times	74.3	55.4	31.9	62.8	38.3	36.4	49.85	+3.90
CARE	\checkmark	\checkmark	74.7	56.8	32.6	62.5	39.7	37.1	50.57	+4.62

listed systems including MiMo-VL-SFT at 81.8 and Qwen3-VL-8B-Thinking at 81.4. On MMMU-Pro_{standard} it attains **46.7**, improving upon the strongest baseline MiMo-VL-7B at 46.2 and all other listed models. The same model also achieves the best score in our suite on MMMU-Pro_{vision} with **41.7**, exceeding MiMo-VL-7B at 40.3 and MiMo-VL-SFT at 39.4. Performance on MATH-Vision_{full} and MMMU_{val} is competitive relative to strong reasoning baselines; on MathVerse_{mini} our method trails the thinking-style decoders but still yields solid gains over RLVR baselines on the same backbone. We show quantitative cases in Section 11.

Backbone scaling. Moving from the 3B and 7B backbones to Qwen3-VL-8B amplifies the benefits of CARE. Relative to Qwen3-VL-8B-Instruct, Qwen3-VL-8B + CARE improves by +4.9 on MathVista_{mini}, +7.6 on MathVerse_{mini}, +7.8 on MATH-Vision_{full}, and +1.4 on MMMU_{val}, while also establishing strong results on the two MMMU-Pro splits.

RLVR baselines. We compare CARE against GRPO, DAPO, and GSPO on the same Qwen2.5-VL-7B backbone. CARE consistently outperforms group-relative RL baselines across datasets. Macro-averaged over the six benchmarks, Qwen2.5-VL-7B + CARE improves over GRPO by **+4.62** points, over DAPO by **+2.27** points, and over GSPO by **+0.70** points; the corresponding macro-average accuracies are 50.57 (CARE) vs. 49.87 (GSPO), 48.30 (DAPO), and 45.95 (GRPO).

Mechanistic signature. CARE predicts $A_{\text{raw}}[y^+] \propto \sqrt{K'}$ and $\bar{A}_{\text{raw}}[y^-] \propto 1/\sqrt{K'}$ (see Equations (9) and (10)). Figure 2 tests these scalings by aggregating groups with realized $K' \in \{2, \dots, 7\}$: we observe clear linear trends consistent with the $\sqrt{K'}/1/\sqrt{K'}$ signature, while the error bars reflect natural variability across prompts. For reference on the full sample, the anchor *and* negative OLS fits yield $R^2 = 0.223/0.555$, and the theory-normalized check $A_{\text{raw}}[y^+]/\sqrt{K'}$ vs. $\hat{\alpha}$ achieves Pearson $r = 0.998$, indicating that residual deviations largely arise from between-

group variation in α rather than a failure of the predicted scalings. *Interpretation.* The $\sqrt{K'}/1/\sqrt{K'}$ law is a direct consequence of z-scoring a two-level mixture with one positive and K' near-miss negatives. Deviations across prompts are primarily driven by between-group variability in α , not by a breakdown of the scaling itself, as indicated by the theory-normalized check $A_{\text{raw}}[y^+]/\sqrt{K'}$ vs. $\hat{\alpha}$.

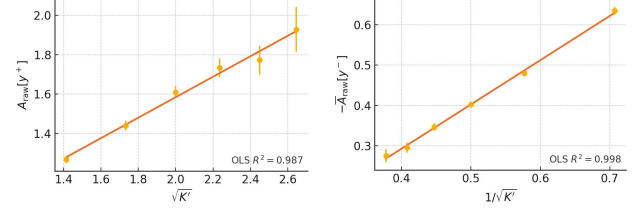


Figure 2. K' signature. Left: $A_{\text{raw}}[y^+]$ vs. $\sqrt{K'}$. Right: $-\bar{A}_{\text{raw}}[y^-]$ vs. $1/\sqrt{K'}$. Markers are bucket means over groups with realized $K' \in \{2, \dots, 7\}$; vertical bars are 95% CIs; solid lines are OLS fits on the means.

4.3. Ablation Study

Ablation on CARE components. Table 2 shows that the anchored-contrastive objective is the primary driver of improvements, while RGR adds a small, consistent boost. Across backbones, the anchored-contrastive objective explains the majority of the macro improvement, while RGR provides a consistent but smaller boost. On Qwen2.5-VL-7B, the macro average rises from 45.95 (GRPO) to 49.85 with *Anchor only* and to 50.57 with *Anchor+RGR*; thus Anchor accounts for 84.4% of the total +4.62 point gain and RGR for the remaining 15.6%. On Qwen2.5-VL-3B, the macro average climbs from 38.83 to 40.15 and then 40.95, so Anchor contributes 62.3% of the +2.12 points and RGR contributes 37.7%. At Figure 3, both CARE variants rise faster than GRPO; the anchored, within-group *z*-scoring with negative-only scaling explains most of this lift. Once

positives become more frequent, RGR triggers and adds a small, steady offset without extra budget. Late in training, CARE shows fewer and shallower dips than GRPO, consistent with lower negative-side clip/variance and the all-negative RESCUE preventing stalls.



Figure 3. We compare **CARE**, **CARE w/o RGR**, and **GRPO** on Qwen2.5-VL-3B. CARE consistently reaches higher reward at matched step budgets; *CARE-wo-RGR* delivers most of the gain, and adding RGR yields a small, consistent, budget-neutral boost.

Ablation on Reflection-Guided Resampling. We test whether the gain of CARE comes from *self-reflection* rather than mere re-sampling. As shown in Figure 4, conditioned on being triggered, RGR achieves a much higher success rate than cue-free controls (76.6% vs 19.3%/12.8%) and correspondingly improves Macro-Average (40.95 vs 39.94/39.76), indicating that the repair cue converts near-miss errors rather than relying on random diversity. Inside each subgroup, anchoring (Section 3.2) yields a stable contrast between the best rollout and K' hard negatives. Guided resampling targets the *failing step* and turns some negatives into stronger positives. For reflected failures, we apply reduced negative-penalty scaling $s_{\text{refl}}=s/2$ in Equation (8) to limit over-sharpening.

Effect of Negative Selection. We isolate the contribution of the negative selector under anchored contrast with within-group z -score normalization (Eqs. (5)–(7)) and cosine distance (Eq. (4)). The left y -axis reports macro-average *Accuracy*; the right y -axis reports the anchor advantage $A_{\text{raw}}[y^+]$. Figure 5 compares COSINE-TOP K' to RANDOM. Starting from identical performance at initialization, COSINE climbs faster and reaches a higher terminal level: it attains ≈ 50.57 , whereas RANDOM plateaus near ≈ 43.06 . Figure 5 further compares NEAREST (top- K' by d_{cos}), MIXED (half nearest + half farthest), and FARTHEST. The ordering is consistent during training and at 6k steps—NEAREST > MIXED > FARTHEST—indicating that mixing or selecting far negatives increases subgroup heterogeneity or provides weak contrast. We therefore adopt COSINE-TOP K' as the default selector.

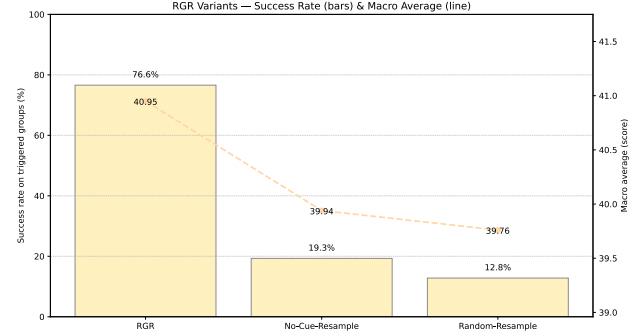


Figure 4. **Reflection success vs. Macro-Average (triggered-only).** *No-Cue-Resample* = resample the same hard negative without the repair prompt; *Random-Resample* = resample without a cue and *not tied* to the original negative. Experiments are built on Qwen2.5-VL-3B.

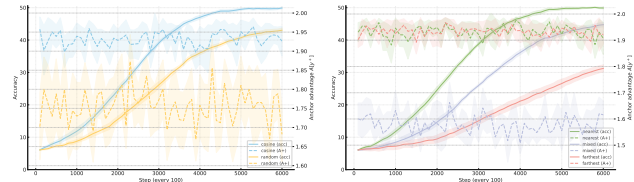


Figure 5. **Left: Cosine vs Random.** Cosine-selected near-miss negatives (COSINE-TOP K') learn substantially faster and converge higher than RANDOM. **Right: Nearest vs Mixed vs Farthest.** Comparing NEAREST (top- K' by d_{cos}), MIXED, and FARTHEST.

Effect of Negative-penalty Scaling. We sweep the negative scaling factor $s \in \{0.7, 0.5, 0.3\}$ against the baseline $s=1.0$ under an identical budget and hyperparameters. To increase sensitivity, we report *stepwise deltas* vs. the baseline for two diagnostics: (i) branch-clip rate on negative-answer tokens; (ii) the variance ratio $R = \text{Var}(A[y^-])/\text{Var}(A[y^+])$, which tests whether scaling acts selectively on negatives. Figure 6 shows two consistent effects: first, the stepwise *delta* branch-clip rate on negative-answer tokens stays mostly below zero and decreases as s becomes smaller, indicating fewer true hits to PPO’s clipped branch exactly where updates are most brittle; second, the stepwise *delta* of the variance ratio R is likewise mostly negative with the same ordering, showing that down-weighting acts *selectively* on negatives rather than shrinking both sides. Together these results substantiate our claim that negative-penalty scaling in Equation (8) stabilizes learning by suppressing negative-side over-updates.

Effect of All-Negative Rescue. We ablate RESCUE by toggling it *ON/OFF* under a shared all-negative trigger and, for each triggered step, compute a triggered-only accuracy gain over the next $B=50$ steps ($\Delta\text{Acc}@B$) together with the per-step update magnitude (ΔKL), presenting both in Figure 7. Compared with OFF, RESCUE=ON shifts the

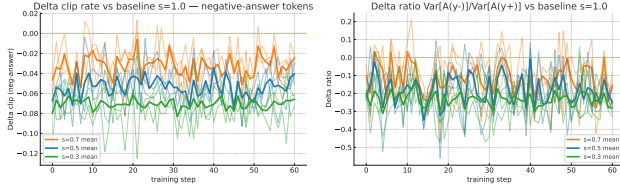


Figure 6. Left: Stepwise *delta* of the branch-clip rate on negative-answer tokens relative to the $s=1.0$ baseline (x-axis: training step ($\times 100$); y-axis: Δ clip). Right: Stepwise *delta* of the variance ratio $\text{Var}(A[y^-])/\text{Var}(A[y^+])$ relative to the $s=1.0$ baseline (x-axis: training step ($\times 100$); y-axis: Δ ratio).

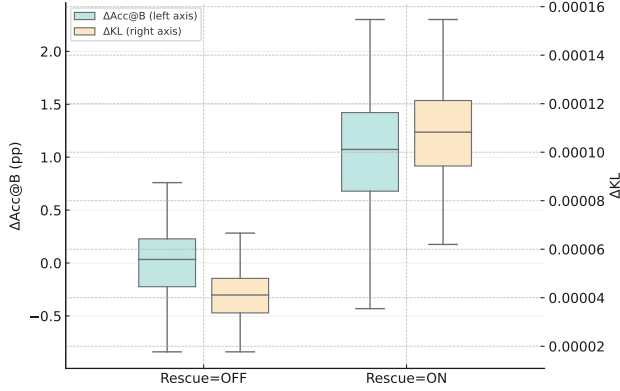


Figure 7. Dual-axis boxplot comparing RESCUE=OFF/ON on all-negative steps under matched decoding budgets. Left axis: $\Delta\text{Acc}@B$ (percentage points); right axis: ΔKL .

entire $\Delta\text{Acc}@B$ distribution upward and lifts ΔKL from near-zero to small, consistent values, indicating that rescue converts stalled hard batches into short-horizon progress without increasing test-time cost.

Effect of Region-Weighted Objective. To isolate sample efficiency, we match runs by cumulative decoded *output* tokens ($T^{\text{out}} = T^{\text{think}} + T^{\text{answer}}$, prompt tokens excluded), start all curves from the same SFT checkpoint with identical decoding, and evaluate on a shared budget grid. Resamples from RGR are counted in the same budget, and all hyperparameters are held fixed so that only region weights differ: *GRPO* (token-uniform), *Answer-only* (answer = 1, all $\langle\text{think}\rangle = 0$), *Region-weighted* (*RW*, $\gamma^+ = 0.005$) (answer = 1, positive $\langle\text{think}\rangle = \gamma^+$, negative/RGR-fail $\langle\text{think}\rangle = 0$), and *RW (fail-think unmasked)* (failing $\langle\text{think}\rangle$ also weighted by γ^+). Under compute parity, *RW* is consistently left-shifted: for any fixed accuracy target it requires fewer tokens, achieves a larger area-under-curve, and attains a higher late-stage plateau—about 3 points above the strongest baseline at the final budget. The unmasked variant underperforms *RW*, indicating that granting gradient credit to failing $\langle\text{think}\rangle$ injects harmful signal and slows learning; *GRPO* lags due

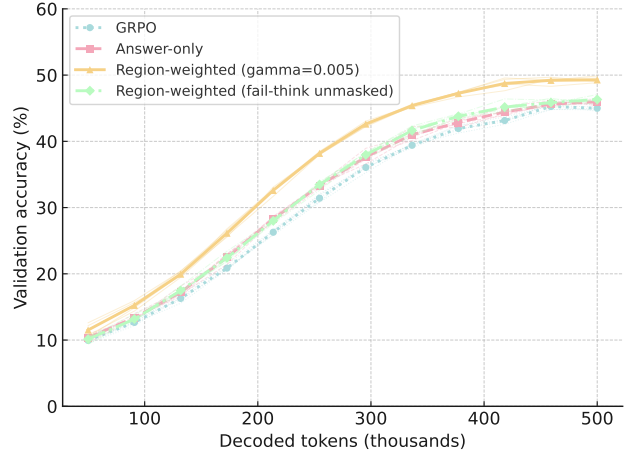


Figure 8. **Accuracy vs decoded tokens.** All curves begin near 6% accuracy; the *Region-weighted* ($\gamma^+ = 0.005$) curve reaches about 50% at the final budget, while *GRPO*, *Answer-only*, and *Region-weighted (fail-think unmasked)* end around 46–47%. Thin lines show per-seed runs and markers show seed means; no smoothing or error bars.

to answer-credit dilution over long rationales, while *Answer-only* discards useful positive-rationale signal and saturates lower.

Further ablations. Additional controls (e.g., trigger sensitivity, selector hyperparameters M/K , and decoding settings) are provided in Appendix Section 9.

5. Conclusion

We recast verifiable-reward post-training as *learning from failures*. Under an unchanged single-decode evaluation protocol, CARE turns near-miss errors into supervision through three lightweight ingredients: (i) an anchored, subgroup-normalized contrast with negative-only scaling that separates correct solutions from plausible failures; (ii) a *training-only*, success-conditioned Reflection-Guided Resampling that attempts a single structured repair on a representative hard negative; and (iii) an all-negative, zero-sum rescue together with region-weighted token credit. This design preserves inference cost while stabilizing group-relative updates.

Across MathVista, MathVerse, MATH-Vision, MMMU, and MMMU-Pro, CARE improves exact-match accuracy and training smoothness—e.g., +4.62 macro points over GRPO on Qwen2.5-VL-7B—and attains the strongest numbers in our reproducible setting on MathVista and MMMU-Pro with Qwen3-VL-8B. We defer limitations and future directions to Appendix Sec. 10.

References

- [1] Arash Ahmadian, Chris Cremer, Matthias Gallé, Marzieh Fadaee, Julia Kreutzer, Olivier Pietquin, Ahmet Üstün, and Sara Hooker. Back to basics: Revisiting reinforce-style optimization for learning from human feedback in llms. In *ACL*, 2024. [2](#)
- [2] Xiang An, Yin Xie, Kaicheng Yang, Wenkang Zhang, Xiuwei Zhao, Zheng Cheng, Yirui Wang, Songcen Xu, Changrui Chen, Chunsheng Wu, et al. Llava-onevision-1.5: Fully open framework for democratized multimodal training. *arXiv preprint arXiv:2509.23661*, 2025. [5](#)
- [3] Anthropic. Claude 3.7 sonnet and claude code. <https://www.anthropic.com/news/claude-3-7-sonnet>, 2025. [5](#)
- [4] Shuai Bai, Keqin Chen, Xuejing Liu, Jialin Wang, Wenbin Ge, Sibo Song, Kai Dang, Peng Wang, Shijie Wang, Jun Tang, et al. Qwen2.5-vl technical report. *arXiv preprint arXiv:2502.13923*, 2025. [5](#)
- [5] Junming Chen, Guang Li, Yiming Chen, Yuzhe Zhong, Yue Wang, Yan Song, Dahua Lin, and Hanwang Zhang. M³cot: A novel benchmark for multi-domain multi-step multi-modal chain-of-thought. In *ACL*, 2024. [3](#)
- [6] Shuang Chen, Yue Guo, Yimeng Ye, Shijue Huang, Wenbo Hu, Haoxi Li, Manyuan Zhang, Jiayu Chen, Song Guo, and Nanyun Peng. Ares: Multimodal adaptive reasoning via difficulty-aware token-level entropy shaping. *arXiv preprint arXiv:2510.08457*, 2025. [2](#)
- [7] DeepSeek-AI, Daya Guo, Dejian Yang, Haowei Zhang, Junxiao Song, Ruoyu Zhang, Runxin Xu, Qihao Zhu, Shirong Ma, Peiyi Wang, et al. Deepseek-r1: Incentivizing reasoning capability in llms via reinforcement learning. *arXiv preprint arXiv:2501.12948*, 2025. [2](#)
- [8] Kaixuan Fan, Kaituo Feng, Haoming Lyu, Dongzhan Zhou, and Xiangyu Yue. Sophiav1-r1: Reinforcing mllms reasoning with thinking reward. 2025. [2](#)
- [9] FanqingM. Mmk12. Hugging Face Datasets, 2025. [3](#)
- [10] Demis Hassabis, Koray Kavukcuoglu, and Gemini Team. Introducing gemini 2.0: A new ai model for the agentic era. <https://blog.google/technology/google-deepmind/google-gemini-ai-update-december-2024/>, 2024. [5](#)
- [11] Zhuoyang He, Huazhe Liu, Yang Gao, and Xiaolong Sun. Seephys: A benchmark for visual physical reasoning. 2025. [3](#)
- [12] Wenxuan Huang, Bohan Jia, Zijie Zhai, Shaosheng Cao, Zheyu Ye, Fei Zhao, Yao Hu, and Shaohui Lin. Vision-r1: Incentivizing reasoning capability in multimodal large language models. 2025. [2, 3, 5](#)
- [13] Kwai Keye Team, Biao Yang, Bin Wen, Changyi Liu, Chenguang Chu, Chengru Song, Chongling Rao, Chuan Yi, Da Li, Dunju Zang, et al. Kwai keye-vl technical report. *arXiv preprint arXiv:2507.01949*, 2025. [5](#)
- [14] Sicong Leng, Jing Wang, Jiaxi Li, Hao Zhang, Zhiqiang Hu, Boqiang Zhang, Yuming Jiang, Hang Zhang, Xin Li, Lidong Bing, Deli Zhao, Wei Lu, Yu Rong, Aixin Sun, and Shijian Lu. Mmr1: Enhancing multimodal reasoning with variance-aware sampling and open resources. 2025. [2, 3](#)
- [15] Lei Li, Pengfei Zhan, Yong Zhang, Zhiqiang Yu, Wei Gao, and Dahua Lin. Metaspacial reasoner: Spatially grounded reinforcement learning for multimodal reasoning. 2025. [2](#)
- [16] Rongjie Li, Keke Tang, Xin Zhu, Le Ji, Nan Duan, and Heng Ji. Vtool-r1: Visual tool use via rule-based reinforcement learning. 2025. [3](#)
- [17] Yuting Li, Lai Wei, Kaipeng Zheng, Jingyuan Huang, Linghe Kong, Lichao Sun, and Weiran Huang. Vision matters: Simple visual perturbations can boost multimodal math reasoning. 2025. [3](#)
- [18] Haotian Liu, Chunyuan Li, Qingyang Wu, and Yong Jae Lee. Visual instruction tuning. *arXiv preprint arXiv:2304.08485*, 2023. [2](#)
- [19] Xiangyan Liu, Jinjie Ni, Zijian Wu, Chao Du, Longxu Dou, Haonan Wang, Tianyu Pang, and Michael Qizhe Shieh. Noisyrollout: Reinforcing visual reasoning with data augmentation. 2025. [3](#)
- [20] Zichen Liu, Changyu Chen, Wenjun Li, Penghui Qi, Tianyu Pang, Chao Du, Wee Sun Lee, and Min Lin. Understanding r1-zero-like training: A critical perspective. 2025. [2](#)
- [21] Zhongzhi Liu, Shujian Tang, Yuxin Zhao, Lei Li, Junqi Fan, and et al. Gui-r1: Towards generalist and efficient computer-use agents via reasoning-centric reinforcement learning. 2025. [2](#)
- [22] Pan Lu, Ran Gong, Shibiao Jiang, Liang Qiu, Siyuan Huang, Xiaodan Liang, and Song-Chun Zhu. Inter-gps: Interpretable geometry problem solving with formal language and symbolic reasoning. In *Proceedings of the 59th Annual Meeting of the Association for Computational Linguistics and the 11th International Joint Conference on Natural Language Processing (Volume 1: Long Papers)*, pages 6774–6786, Online, 2021. Association for Computational Linguistics. [5, 2](#)
- [23] Pan Lu, Hritik Bansal, Tony Xia, Jiacheng Liu, Chunyuan Li, Hannaneh Hajishirzi, Hao Cheng, Kai-Wei Chang, Michel Galley, and Jianfeng Gao. Mathvista: Evaluating mathematical reasoning of foundation models in visual contexts. *arXiv preprint arXiv:2310.02255*, 2024. [2, 3, 5](#)
- [24] Ahmed Masry, Do Xuan Long, Jia Qing Tan, Shafiq Joty, and Enamul Hoque. Chartqa: A benchmark for question answering about charts with visual and logical reasoning. In *Findings of the Association for Computational Linguistics: ACL 2022*, pages 2263–2279, Dublin, Ireland, 2022. Association for Computational Linguistics. [5, 2](#)
- [25] MMMU Team. Mmmu: A massive multi-discipline multimodal understanding benchmark. Hugging Face Datasets, 2023. [2, 3, 5](#)
- [26] Youssef Mroueh. Reinforcement learning with verifiable rewards: Grpo's effective loss, dynamics, and success amplification. *arXiv preprint arXiv:2503.06639*, 2025. [2](#)
- [27] OpenAI. Gpt-4v(ision) system card. <https://openai.com/index/gpt-4v-system-card/>, 2023. [2](#)
- [28] OpenAI. Gpt-4o system card. *arXiv preprint arXiv:2410.21276*, 2024. [5](#)
- [29] OpenAI. Gpt-5 nano — model card. <https://platform.openai.com/docs/models/gpt-5-nano>, 2025. [5](#)

[30] Shengju Qian, Hao Shao, Han Xiao, Guanglu Song, Zhuofan Zong, Letian Wang, Yu Liu, and Hongsheng Li. Llava-cot: Let vision-language models reason step-by-step. 2024. 3

[31] Chagai Razin, Rohan Paleja, Jonathan Ho, and Ramin Hasani. Depth-breadth synergy in rlrv: Unlocking llm reasoning gains with difficulty adaptive rollout sampling. 2025. 2

[32] Gabriel Sarch, Snigdha Saha, Naitik Khandelwal, Ayush Jain, Michael J. Tarr, Aviral Kumar, and Katerina Fragkiadaki. Grounded reinforcement learning for visual reasoning. 2025. 2

[33] Zhihong Shao, Peiyi Wang, Qihao Zhu, Runxin Xu, Junxiao Song, Xiao Bi, Haowei Zhang, Mingchuan Zhang, Y. K. Li, Y. Wu, and Daya Guo. Deepseekmath: Pushing the limits of mathematical reasoning in open language models. *arXiv preprint arXiv:2402.03300*, 2024. 2, 5

[34] Xiaolong Su, Haoyu Zhang, Yuxin Li, Xizhou Zhu, and Jifeng Dai. Long-rl: Scaling reinforcement learning for long-horizon video reasoning. 2025. 3

[35] TIGER-Lab. Virl39k. Hugging Face Datasets, 2025. 3

[36] Fudong Wang, Jiajia Liu, Jingdong Chen, Jun Zhou, Kaixiang Ji, Lixiang Ru, Qingpei Guo, Ruobing Zheng, Tianqi Li, Yi Yuan, Yifan Mao, Yuting Xiao, and Ziping Ma. M2-reasoning: Empowering mllms with unified general and spatial reasoning. *arXiv preprint arXiv:2507.08306*, 2025. 5

[37] Haozhe Wang, Chao Qu, Zuming Huang, Wei Chu, Fangzhen Lin, and Wenhui Chen. Vl-rethinker: Incentivizing self-reflection of vision-language models with reinforcement learning. 2025. 2, 5

[38] Ke Wang, Junting Pan, Weikang Shi, Zimu Lu, Mingjie Zhan, and Hongsheng Li. Measuring multimodal mathematical reasoning with math-vision dataset. *arXiv preprint arXiv:2402.14804*, 2024. 2, 3, 5

[39] Ruibin Wang, Shuyue Xu, Lanjun Chen, Yutong Wang, Zhiqiang Wang, Yifan Zhang, Xiaowei Hu, Xiaohong Wang, and Lei Zhang. Editgrpo: Training radiology report generators with verifiable edits and group relative policy optimization. In *MICCAI*, 2024. 3

[40] Weiyun Wang, Zhangwei Gao, Lixin Gu, Hengjun Pu, Long Cui, Xingguang Wei, Zhaoyang Liu, Linglin Jing, Shenglong Ye, Jie Shao, et al. Internvl3.5: Advancing open-source multimodal models in versatility, reasoning, and efficiency. *arXiv preprint arXiv:2508.18265*, 2025. 5

[41] Yishuang Xie, Jiayi Xing, Fangchang Ma, Hui Liu, Yuwei Liu, Hanzhao Wang, Mohit Bansal, Yu Su, Linxi Fan, Ki-hyuk Sohn, Chi Yu, Lijuan Wang, Xiangtao Yang, Steven C. H. Hoi, Humphrey Shi, Yannis Kalantidis, Alexandre Alahi, Hakan Bilen, Zhecan Wang, Junxiong Shen, and Christoph Feichtenhofer. Vppo: Visually-grounded policy optimization for lylms. 2025. 2

[42] An Yang, Anfeng Li, Baosong Yang, Beichen Zhang, Binyuan Hui, Bo Zheng, Bowen Yu, Chang Gao, Chengan Huang, Chenxu Lv, et al. Qwen3 technical report. *arXiv preprint arXiv:2505.09388*, 2025. 5

[43] Yi Yang, Xiaoxuan He, Hongkun Pan, Xiyan Jiang, Yan Deng, Xingtao Yang, Haoyu Lu, Fengyun Rao, Minfeng Zhu, Bo Zhang, and Wei Chen. R1-onevision: Advancing generalized multimodal reasoning through cross-modal formalization. 2025. 3

[44] Qiying Yu, Zheng Zhang, Ruofei Zhu, Yufeng Yuan, Xiaochen Zuo, Yu Yue, Weinan Dai, Tiantian Fan, Gaohong Liu, Lingjun Liu, Xin Liu, Haibin Lin, Zhiqi Lin, Bole Ma, Guangming Sheng, Yuxuan Tong, Chi Zhang, Mofan Zhang, Wang Zhang, Hang Zhu, Jinhua Zhu, Jiangjie Chen, Jiaze Chen, Chengyi Wang, Hongli Yu, Yuxuan Song, Xiangpeng Wei, Hao Zhou, Jingjing Liu, Wei-Ying Ma, Ya-Qin Zhang, Lin Yan, Mu Qiao, Yonghui Wu, and Mingxuan Wang. Dapo: An open-source llm reinforcement learning system at scale. *arXiv preprint arXiv:2503.14476*, 2025. 2, 5

[45] Xiang Yue, Tianyu Zheng, Yuansheng Ni, Yubo Wang, Kai Zhang, Shengbang Tong, Yuxuan Sun, Bota Yu, Ge Zhang, Huan Sun, Yu Su, Wenhui Chen, and Graham Neubig. Mmmu-pro: A more robust multi-discipline multimodal understanding benchmark. *arXiv preprint arXiv:2409.02813*, 2024. 3, 5

[46] Zihao Yue, Zhenru Lin, Yifan Song, Weikun Wang, Shuhuai Ren, Shuhao Gu, Shicheng Li, Peidian Li, Liang Zhao, Lei Li, et al. Mimo-vl technical report. *arXiv preprint arXiv:2506.03569*, 2025. 5

[47] Kaichen Zhang, Bo Li, Peiyuan Zhang, Fanyi Pu, Joshua Adrian Cahyono, Kairui Hu, Shuai Liu, Yuanhan Zhang, Jingkang Yang, Chunyuan Li, and Ziwei Liu. Lmms-eval: Reality check on the evaluation of large multimodal models, 2024. 5

[48] Pengfei Zhang, Guoqiang Zhang, Jie Guo, and Yi Lin. R1-track: Tracking via reinforcement learning for long-horizon reasoning. 2025. 3

[49] Renrui Zhang, Dongzhi Jiang, Yichi Zhang, Haokun Lin, Ziyu Guo, Pengshuo Qiu, Aojun Zhou, Pan Lu, Kai-Wei Chang, Peng Gao, and Hongsheng Li. Mathverse: Does your multi-modal llm truly see the diagrams in visual math problems? *arXiv preprint arXiv:2403.14624*, 2024. 2, 3, 5

[50] Chujie Zheng, Shixuan Liu, Mingze Li, Xiong-Hui Chen, Bowen Yu, Chang Gao, Kai Dang, Yuqiong Liu, Rui Men, An Yang, Jingren Zhou, and Junyang Lin. Group sequence policy optimization. 2025. 2, 5

[51] Ziwei Zheng, Michael Yang, Jack Hong, Chenxiao Zhao, Guohai Xu, Le Yang, Chao Shen, and Xing Yu. Deep-eyes: Incentivizing “thinking with images” via reinforcement learning. *arXiv preprint arXiv:2505.14362*, 2025. 5

CARE What Fails: Contrastive Anchored-Reflection for Verifiable Multimodal Reasoning

Supplementary Material

6. Notation

Sym.	Meaning
x	Multimodal input instance.
\mathbf{I}	Image or set of images in the input.
\mathbf{q}	Text query in the input.
π_θ	Trainable policy that generates rationale and answer.
\hat{r}	Rationale inside the <code><think></code> span.
\hat{y}	Final answer inside the <code><answer></code> span.
\mathcal{V}	Programmatic verifier of answers.
acc	Verifier accuracy signal.
fmt	Verifier format-compliance signal.
r	Overall reward signal.
r_i	Reward assigned to the i -th rollout.
y	A model response.
y_i	The i -th rollout for a given input.
\mathcal{Y}	Collection of rollouts for a given input.
G	Number of rollouts sampled per input.
T_i	Total token count of the i -th response.
T_i^{ans}	Token count inside the answer span of the i -th response.
T_i^{think}	Token count inside the rationale span of the i -th response.
\mathcal{P}	Indices of verifier-positive rollouts.
y^+	Anchor rollout selected from verifier-positive rollouts.
\mathcal{F}	Failure pool of verifier-negative rollouts.
\mathcal{N}	Selected hard negatives.
K	Target number of negatives in the subgroup.
K'	Realized number of negatives in the subgroup.
S	Anchored subgroup used for normalization and updates.
S^*	Indices with nonzero sequence-level advantages.
M	Preselection size before diversity pruning among negatives.
\tilde{h}_i	Normalized rationale embedding of the i -th rollout.
\tilde{h}_+	Normalized rationale embedding of the anchor.
d_{cos}	Cosine-distance metric in the embedding space.
μ_S	Mean reward within the subgroup.
σ_S	Standard-deviation scale within the subgroup.
$A[y]$	Sequence-level advantage for a rollout.
s	Scaling factor applied to negative advantages.
s_{refl}	Reduced scaling factor for failed reflection samples.
$\rho_{i,t}$	Importance ratio at token position t for the i -th rollout.
$w_{i,t}$	Region weight at token position t for the i -th rollout.
γ^+	Weight for rationale tokens of verifier-positive samples.
$a_{i,t}$	Per-token advantage at position t for the i -th rollout.
ε	Small constant for numerical stabilization.
ϵ_w	Small constant used in token-level normalization.
ϵ_{low}	Lower clipping threshold in the surrogate objective.
ϵ_{high}	Upper clipping threshold in the surrogate objective.
π_{old}	Behavior policy used for importance ratios.
π_{ref}	Reference policy used in KL regularization.
β	Coefficient of the KL regularizer.
y^-	Hard negative used for reflection-guided resampling.
RGR	Reflection-Guided Resampling procedure.
δ	Magnitude used in the all-negative rescue pseudo-contrast.
t	Pseudo-anchor used in the all-negative rescue.
r^+	Reward of the anchor rollout.
m_-	Mean reward among negatives in the subgroup.
Δ	Reward gap between the anchor and negatives.
Var_-	Reward variance among negatives in the subgroup.
α	Attenuation factor in the mechanistic analysis.

Table 3. **Notation.** Single-symbol entries with descriptions that avoid formulas.

7. Proof of K Mechanistic signature

Setup. Let the anchored subgroup be $S = \{y^+\} \cup \{y_1^-, \dots, y_{K'}^-\}$. The anchor has reward r^+ ; negatives are i.i.d. with mean m_- and variance Var_- . Define $\Delta = r^+ - m_- > 0$. Advantages are group-normalized as in Eqs. (5) to (7) (we drop the tiny ε for clarity).

Proposition 1 (Two-level K -signature under small dispersion). *Under the assumptions above, a plug-in (delta-method) approximation that replaces the random denominator by $\sqrt{\mathbb{E}[\sigma_S^2]}$ yields*

$$\mathbb{E} A[y^+] \approx \alpha_{K'} \sqrt{K'}, \quad \mathbb{E} \bar{A}[y^-] \approx -\alpha_{K'} \frac{1}{\sqrt{K'}},$$

where

$$\alpha_{K'} = \frac{\Delta}{\sqrt{K' \text{Var}_- + \Delta^2}} \in (0, 1].$$

Sketch. We have $\mathbb{E}[\mu_S] = m_- + \frac{\Delta}{K'+1}$ and

$$\begin{aligned} \mathbb{E}[(r^+ - \mu_S)^2] &= \frac{K'^2}{(K'+1)^2} \Delta^2 \\ &\quad + \frac{K'}{(K'+1)^2} \text{Var}_-. \end{aligned}$$

Similarly,

$$\begin{aligned} \mathbb{E}[(r_j^- - \mu_S)^2] &= \text{Var}_- \left(1 - \frac{2}{K'+1} + \frac{K'}{(K'+1)^2} \right) \\ &\quad + \frac{\Delta^2}{(K'+1)^2}. \end{aligned}$$

Therefore

$$\begin{aligned} \mathbb{E}[\sigma_S^2] &= \frac{1}{K'+1} \left(\mathbb{E}[(r^+ - \mu_S)^2] + K' \mathbb{E}[(r_j^- - \mu_S)^2] \right) \\ &= \frac{K'^2}{(K'+1)^2} \text{Var}_- + \frac{K'}{(K'+1)^2} \Delta^2. \end{aligned}$$

Also $\mathbb{E}[r^+ - \mu_S] = \frac{K'}{K'+1} \Delta$. Approximating $\mathbb{E}[(r^+ - \mu_S)/\sigma_S] \approx \mathbb{E}[r^+ - \mu_S]/\sqrt{\mathbb{E}[\sigma_S^2]}$ gives

$$\begin{aligned} \mathbb{E} A[y^+] &\approx \frac{\Delta \frac{K'}{K'+1}}{\sqrt{\frac{K'^2}{(K'+1)^2} \text{Var}_- + \frac{K'}{(K'+1)^2} \Delta^2}} \\ &= \frac{\Delta \sqrt{K'}}{\sqrt{K' \text{Var}_- + \Delta^2}} = \alpha_{K'} \sqrt{K'}. \end{aligned}$$

For a negative y_j^- , $\mathbb{E}[r_j^- - \mu_S] = -\frac{\Delta}{K'+1}$, which yields the stated $\mathbb{E} \bar{A}[y^-]$. \square

Corollary 1 (Binary rewards). *If $r^+ = 1$ and all negatives satisfy $r_j^- = 0$ (i.e., $\text{Var}_- = 0$, $\Delta = 1$), then the z-scored advantages are exact:*

$$A[y^+] = \sqrt{K'}, \quad A[y_j^-] = -\frac{1}{\sqrt{K'}},$$

matching Eq. (10).

Corollary 2 (All-negative Rescue). *Under the pseudo-reward assignment in Eq. (14) on $S = \{t\} \cup \mathcal{N}$, with $r'[t] = \delta$, $r'[j] = -\delta/K'$ for $j \in \mathcal{N}$, we have $\mu_S = 0$ and*

$$\sigma_S^2 = \frac{\delta^2}{K'}.$$

Hence

$$A[t] = \sqrt{K'}, \quad A[j] = -\frac{1}{\sqrt{K'}}.$$

Thus the rescue update reproduces the $\sqrt{K'}$ signature exactly.

8. Implementation Details

8.1. Datasets Details

We build our visual reasoning training set by pooling three publicly available sources—ChartQA [24], Geometry3K [22], and ViRL39K [37]. All examples are standardized into a unified image–prompt–answer schema, followed by light cleaning and cross-corpus deduplication. The merged collection contains approximately **49.3K** unique multimodal prompts. Table 4 summarizes the per-source counts and shares prior to merging: **7,398** from ChartQA (15.3%), **2,101** from Geometry3K (4.3%), and **38,870** from ViRL39K (80.4%), totaling **48,369** items. This mixture provides complementary coverage of chart reasoning, geometric diagram understanding, and broader visual reasoning.

Table 4. Sources and sizes of the visual reasoning training set.

Dataset	Reference	Count	Share
ChartQA	[24]	7,398	15.3%
Geometry3K	[22]	2,101	4.3%
ViRL39K	[37]	38,870	80.4%
Total		48,369	100.0%

8.2. Experimental Details

Sampling and groups. Unless otherwise noted, we sample $G=8$ rollouts per prompt for all methods. For CARE, we form an anchor-aware hard-negative subgroup of size $K=4$ (Sections 3.2 and 3.3). In all main results we set $M = 6$. Within each subgroup we compute group-normalized advantages (Section 3.4); negatives are

down-weighted by the factor $s=0.5$ (Eq. (8)). When a verifier-positive anchor exists, Reflection-Guided Resampling (RGR; Section 3.6) performs one training-only resample on the selected hard negative; reflected failures are further reduced by $s_{\text{refl}}=s/2$. In all-negative groups we enable the *Rescue* mechanism with pseudo-contrast magnitude $\delta=0.1$ (Section 3.7). Region weights follow Equation (11) with $\gamma^+=0.005$ for positive `<think>` (note: `<reasoning>` with Qwen3VL-8B) tokens and 0 on negatives; answer tokens always receive weight 1.

Optimization. All methods use the same PPO-style clipped objective (Equation (12)) with a fixed KL regularizer to a reference policy (Equation (13)). Decoding hyperparameters (e.g., temperature, nucleus/top- p) are held constant across methods and reused at evaluation; inference always uses a *single* decode and *no* reflection.

Baselines and fairness. We re-train GRPO [33], DAPO [44], and GSPO [50] on the same 49.3K mixture with the same rollout budget $G=8$, identical decoding, and a matched optimization budget (steps, tokens, and KL schedule). Baselines keep their standard token-uniform weighting (no region weighting) and do not use reflection. All models—ours and baselines—are trained from the same SFT cold-start and use the same verifier signals acc and fmt combined by Eq. (1).

Seeds and reporting. Unless stated otherwise, we train with $n=5$ independent random seeds and report the mean; 95% confidence intervals are $\bar{x} \pm 1.96 \sigma / \sqrt{n}$ and shown in figures/tables where space permits.

8.3. Evaluation Details

Common protocol. All evaluations use a *single* decode per example under identical decoding hyperparameters for every model. We extract the text inside the `<answer>...</answer>` span and compute *exact match* against the benchmark’s key using the official normalization rules (no custom post-processing). Scores are reported per benchmark; the *macro average* is the unweighted mean across all six benchmarks. The open-ended answers of benchmarks are judged by GPT-5.

MathVista_{mini} [23] targets mathematical and scientific reasoning with plots, charts, and diagrams; answers are short and programmatically verifiable.

MathVerse_{mini} [49] covers math-intensive visual problems (algebra/geometry/physics) presented as figures or rendered text-in-image.

MATH-Vision_{full} [38] evaluates multi-step math reasoning grounded in images (e.g., annotated diagrams); answers are discrete and exact-matchable.

Algorithm 1 CARE: Anchored-Contrastive Objective with Reflection-Guided Resampling (updated)

Require: input x ; policy π_θ ; old policy π_{old} ; reference π_{ref} ; rollout budget G ; target subgroup size K ; neg_scale s ; reduced neg_scale $s_{\text{refl}} \leq s$; answer/rationale weight γ^+ ; reward mix $\lambda \in [0, 1]$; clipping $(\epsilon_{\text{low}}, \epsilon_{\text{high}})$; KL coef β ; normalization constants ε, ϵ_w ; rescue magnitude δ

1: Sample G rollouts $\mathcal{Y} = \{y_i\}_{i=1}^G$; parse `<think>` and `<answer>` spans; record lengths $T_i^{\text{think}}, T_i^{\text{ans}}$
2: For each y_i : compute verifier signals $(\text{acc}_i, \text{fmt}_i) \leftarrow \mathcal{V}(\text{extract_answer}(y_i))$; set $r_i \leftarrow (1 - \lambda) \text{acc}_i + \lambda \text{fmt}_i$
3: Define $\mathcal{P} \leftarrow \{i : \text{acc}_i = 1\}$ (positives), $\mathcal{F} \leftarrow \{i : \text{acc}_i = 0\}$ (failures)

4: **if** $\mathcal{P} \neq \emptyset$ **then** \triangleright non-all-negative group
5: $a \leftarrow y^+ \leftarrow \arg \min_{i \in \mathcal{P}} (T_i^{\text{think}}, T_i^{\text{ans}})$ \triangleright anchor = shortest `<think>`, tie-break shorter answer
6: $K' \leftarrow \min(K, |\mathcal{F}|)$
7: **if** $K' = 0$ **then skip update and continue** \triangleright all-positive \rightarrow avoid arbitrary drift
8: **end if**
9: $\mathcal{N} \leftarrow \text{AnchorAwareNegatives}(\mathcal{F}, K', y^+)$ \triangleright rank failures by cosine to anchor's `<think>` embedding; stop-gradient; brief farthest-first de-dup
10: $S \leftarrow \{y^+\} \cup \{y_1^-, \dots, y_{K'}^-\}; \tilde{r}(y) \leftarrow r(y)$
11: **if** reflection enabled **then** \triangleright Reflection-Guided Resampling (train-time only)
12: Choose $y^{\text{neg}} \in \mathcal{N}$ (e.g., hardest by d_{cos})
13: Insert concise repair cue into `<think>` of y^{neg} , decode once to obtain y^{rgr}
14: Parse y^{rgr} ; compute $(\text{acc}_{\text{rgr}}, \text{fmt}_{\text{rgr}})$, $r_{\text{rgr}} \leftarrow (1 - \lambda) \text{acc}_{\text{rgr}} + \lambda \text{fmt}_{\text{rgr}}$
15: **if** $\text{acc}_{\text{rgr}} = 1$ **then** \triangleright success defined by verifier-positive
16: $S \leftarrow (S \setminus \{y^{\text{neg}}\}) \cup \{y^{\text{rgr}}\}; \tilde{r}(y^{\text{rgr}}) \leftarrow r_{\text{rgr}}$
17: **else** \triangleright reflection fails
18: $S \leftarrow S \cup \{y^{\text{rgr}}\}; \tilde{r}(y^{\text{rgr}}) \leftarrow r_{\text{rgr}}$; mark y^{rgr} for reduced scaling s_{refl}
19: **end if**
20: **end if**
21: **else** \triangleright all-negative group
22: $t \leftarrow \text{ProxyAnchor}(\mathcal{F}) \equiv \arg \max_{i \in \mathcal{F}} \log \pi_{\text{old}}(y_i | x)$
23: $K' \leftarrow \min(K, |\mathcal{F}|); \mathcal{N} \leftarrow \text{AnchorAwareNegatives}(\mathcal{F} \setminus \{t\}, K', t)$
24: $S \leftarrow \{t\} \cup \mathcal{N}$; assign pseudo-rewards on S : $\tilde{r}(t) \leftarrow \delta$, $\tilde{r}(j) \leftarrow -\delta/K'$ for $j \in \mathcal{N}$; $a \leftarrow t$
25: **end if**
26: $K_S \leftarrow |\{y \in S \setminus \{a\} : \tilde{r}(y) < \tilde{r}(a)\}|$ \triangleright negatives actually present after any reflection
27: **if** $K_S = 0$ **then skip update and continue**
28: **end if**
29: $\mu_S \leftarrow |S|^{-1} \sum_{y \in S} \tilde{r}(y); \sigma_S \leftarrow \sqrt{|S|^{-1} \sum_{y \in S} (\tilde{r}(y) - \mu_S)^2} + \varepsilon$
30: Initialize $A(y) \leftarrow 0$ for all $y \in \mathcal{Y}$ (and any reflected sample)
31: **for** each $y \in S$ **do**
32: $A_{\text{raw}}(y) \leftarrow (\tilde{r}(y) - \mu_S)/\sigma_S$
33: **end for**
34: Set $A(a) \leftarrow A_{\text{raw}}(a)$
35: **for** each $y \in S \setminus \{a\}$ **do**
36: $s_y \leftarrow s$; **if** y is a failed reflected sample **then** $s_y \leftarrow s_{\text{refl}}$
37: $A(y) \leftarrow -s_y |A_{\text{raw}}(y)|$
38: **end for**
39: **Equalize update size:** **if** $K_S < K$ **then** $A(\cdot) \leftarrow \sqrt{K/K_S} A(\cdot)$
40: **Region weights:** for token t in y_i :
 $w_{i,t} = 1$ if $t \in \text{answer}$; $w_{i,t} = \gamma^+$ if $t \in \text{think}$ and $\text{acc}_i = 1$; $w_{i,t} = 0$ if $t \in \text{think}$ and $\text{acc}_i = 0$
41: Per-token advantage $a_{i,t} \leftarrow A[y_i] \cdot \frac{w_{i,t}}{\sum_{u=1}^{T_i} w_{i,u} + \epsilon_w}$
42: PPO loss with clipping:

$$\mathcal{L}_{\text{PG}} = -\frac{1}{|S^*|} \sum_{i \in S^*} \sum_t \min \left\{ \rho_{i,t} a_{i,t}, \text{clip}(\rho_{i,t}, 1 - \epsilon_{\text{low}}, 1 + \epsilon_{\text{high}}) a_{i,t} \right\},$$
 where $S^* = \{i : A[y_i] \neq 0\}$ and $\rho_{i,t} = \exp(\log \pi_\theta - \log \pi_{\text{old}})$
43: Add KL regularizer: $\mathcal{L} \leftarrow \mathcal{L}_{\text{PG}} + \beta \text{KL}[\pi_\theta \parallel \pi_{\text{ref}}]$; update $\theta \leftarrow \theta - \eta \nabla_\theta \mathcal{L}$

MMMU_{val} [25] spans multi-disciplinary, multi-image questions; we report accuracy on the public validation set.

MMMU- $\text{Pro}_{\text{standard}}$ and **MMMU- $\text{Pro}_{\text{vision}}$** [45] evaluate professional-level reasoning, with the *vision* split focus-

Table 5. Training-time configuration (shared vs. method-specific). “Uniform” = token-uniform weighting; “RW” = region-weighted scheme in Eq. (11).

Method	G	K	Neg. scale	Rescue	Reflection (train)	Token weights	Clip_{low}	$\text{Clip}_{\text{high}}$	$\text{KL coef } \beta$
CARE (ours)	8	4	$s=0.5$	$\delta=0.1$	Yes (1 resample)	RW ($\gamma^+=0.005$)	0.20	0.28	0.02
CARE w/o RGR	8	4	$s=0.5$	$\delta=0.1$	No	RW ($\gamma^+=0.005$)	0.20	0.28	0.02
GRPO	8	—	—	—	No	Uniform	0.20	0.20	0.02
DAPO	8	—	—	—	No	Uniform	0.20	0.28	-
GSPO	8	—	—	—	No	Uniform	3e-4	4e-4	-

Shared across all methods unless noted: same data, verifier, and decoding.

ing more heavily on visual content. Both provide deterministic answer keys for exact-match evaluation.

9. Additional Ablations

9.1. Ablation on K and Equalization

We record **Val-Acc** and **KL/step** every 100 training steps. Figures Figures 9 and 10 depict the trajectories. All configurations start near $\approx 17\%$ accuracy and differ only in the subgroup size $K \in \{2, 4, 6\}$ and whether update-size equalization $\sqrt{K/K'}$ (Eq) is enabled. Across the board, enabling Eq accelerates accuracy growth and yields higher final performance while simultaneously lowering and stabilizing KL. The strongest setting is $K=4$ with Eq enabled, converging at $\approx 61.5\%$ versus 59.8% without Eq; similar but slightly smaller gains appear for $K=2$ (57.8% vs. 56.8%) and $K=6$ (60.3% vs. 58.5%). The KL trajectories mirror these patterns: for $K=4$, the final KL drops from ≈ 0.70 (Eq off) to ≈ 0.48 (Eq on); for $K=6$, from ≈ 0.72 to ≈ 0.50 ; and for $K=2$, from ≈ 0.75 to ≈ 0.50 . We also observe narrower confidence intervals with Eq on throughout most of training, indicating reduced seed-to-seed variance and fewer regressions. These results are consistent with the mechanism that the realized hard-negative count K' often falls below K : without equalization the effective update magnitude shrinks whenever $K' < K$, slowing progress and increasing volatility, whereas the $\sqrt{K/K'}$ factor restores a comparable update scale and produces steadier policy updates, reflected in both faster accuracy gains and smoother, lower KL. Taken together, the Acc–KL trade-off favors $K=4$ with Eq on as a robust default; larger K remains competitive provided Eq is enabled, while smaller K is viable under tight budgets but saturates lower.

9.2. Ablation Analysis on Anchor

Holding accuracy approximately constant between the two anchor rules, we still observe a clear separation in reasoning length: with the same initial average think length at initialization, the *Shortest-Think* anchor shortens the average think tokens markedly faster than a *Random* anchor

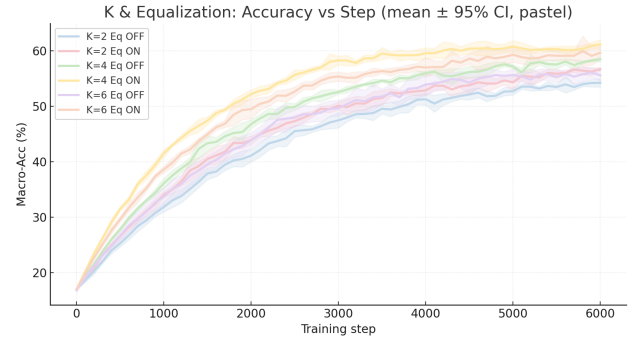


Figure 9. Val-Acc every 100 steps for $K \in \{2, 4, 6\}$ with/without equalization.

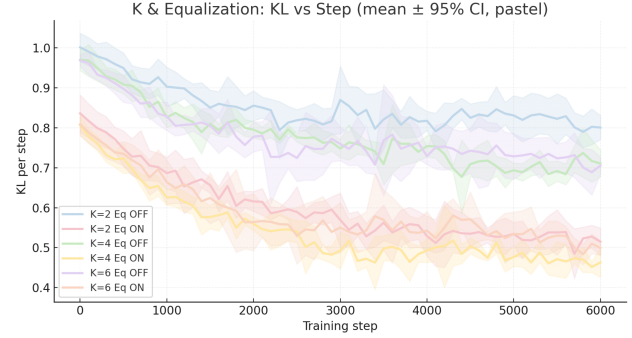


Figure 10. KL per 100 steps.

(Figure 11). By the end of training the gap stabilizes at roughly 15–20 tokens, indicating that the model produces more compact rationales without sacrificing task accuracy. This pattern is consistent with our mechanism: choosing a concise, verifier-positive anchor concentrates the contrast on near-miss negatives and reduces credit dilution in the rationale region, yielding cleaner reasoning at comparable accuracy. Taken together, these results demonstrate that the anchoring rule controls how efficiently learning signal is allocated to the rationale; *Shortest-Think* achieves shorter, more focused reasoning while maintaining the same accu-

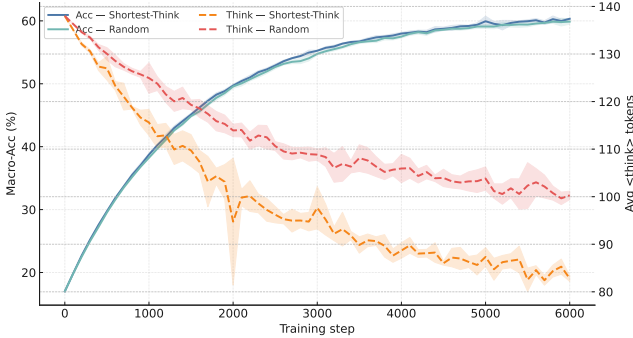


Figure 11. Val-Accuracy and Thinking token length of *Shortest-Think* and *Random* Anchor selection.

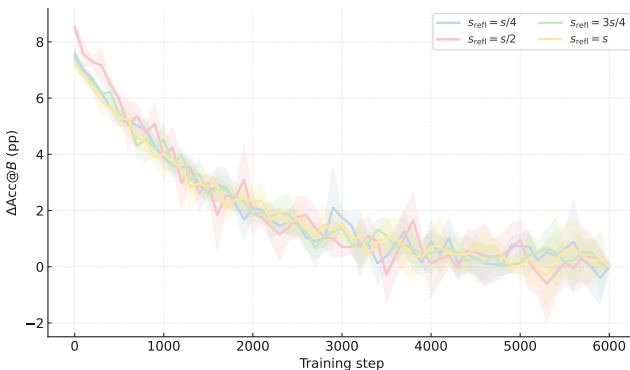


Figure 12. Across training, ACC@300 on different s_{refl} scale.

racy as *Random*.

9.3. Ablation Analysis on s reflection

As shown in Figure 12, across training, we observe a consistent ordering: $s_{\text{refl}} = s/2$ yields the largest per-trigger gain, $3s/4$ is close but lower, while $s/4$ and s lag behind. Early in training (≈ 0 – 2 k steps) the $s/2$ curve rises faster; mid-training (≈ 2 k– 4 k) its advantage persists with narrower confidence bands; late in training all curves flatten but $s/2$ remains on top. This pattern matches the mechanism-level intuition: too small a scaling ($s/4$) under-penalizes failed reflections and does not sufficiently move the policy off the error mode; too large a scaling (s) overshoots and increases brittleness; a moderate scaling ($s/2$) balances gradient magnitude and exploration radius, keeping updates within a repairable neighborhood and converting more hard errors into measurable short-horizon accuracy. We therefore adopt $s_{\text{refl}} = s/2$ as the default choice.

10. Future Directions and Limitations

10.1. Limitations

While CARE demonstrates strong robustness on verifiable reasoning tasks, its current reliance on binary correctness

signals restricts its primary application to domains with objective ground truths, such as mathematics and coding, leaving the extension to open-ended generation contingent on the development of reliable reward models. Additionally, although the all-negative rescue mechanism effectively mitigates gradient collapse in sparse-reward scenarios, the framework operates most efficiently when the policy can discover at least one successful rollout to anchor the contrastive update, implying that extremely hard tasks with near-zero pass rates may still benefit from initial warm-up supervision. Finally, our heuristic preference for the shortest successful rationale is a deliberate design choice to optimize inference efficiency; while this successfully curbs verbosity, it entails a trade-off that may theoretically discourage extended reasoning chains in specific edge cases where exhaustive self-verification is strictly necessary.

10.2. Future Directions

Step-level verification and credit. Augment the reward with *intermediate* verifiers that check sub-goals (e.g., variable extraction, unit conversion, geometric equivalences), enabling token- or span-level advantages on $\langle \text{think} \rangle$ without relying on a global scalar.

Multi-anchor or anchor ensembles. Replace the single anchor with a *set* of diverse positives (e.g., by clustering successful rationales) and distribute positive credit across them. This can mitigate brevity bias, preserve solution diversity, and improve stability on multi-modal prompts with several correct styles.

Learned negative selection. Move beyond cosine heuristics by training a selector that predicts “fixability” or causal proximity to the anchor (e.g., via contrastive learning on success/failure edits). Hybrid selectors could balance semantic proximity with coverage of distinct error families.

Adaptive subgroup sizing and scaling. Learn K' and the negative scaling s from data (or schedule them dynamically) to maintain a target signal-to-noise ratio inside the subgroup. This could reduce sensitivity to class imbalance and reward variance across prompts.

11. Quantitative Case Studies

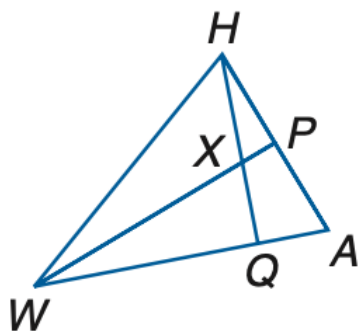
We present detailed case studies illustrating the components of the CARE training objective. For each example, we show:

1. **The Anchor (y^+):** The shortest successful rollout used as the positive reference.
2. **Hard Negatives (y^-):** Failed rollouts selected by cosine similarity. Note how the reasoning traces are semantically close to the anchor (e.g., correct formulas or data

extraction steps) but fail due to specific hallucinations or omissions.

3. **RGR Success:** A sample where the model, prompted with the repair cue, successfully corrects a hard negative.

Case 1: Geometry



Question: If \overline{WP} is a perpendicular bisector, $m\angle WHA = 8q + 17$, $m\angle HWP = 10 + q$, $AP = 6r + 4$, and $PH = 22 + 3r$, find q .

GT Answer: 7

1. Anchor (y^+) [Positive]

Shortest correct reasoning path.

<think> $\overline{WP} \perp \overline{HA} \implies \angle WPH = 90^\circ$. In $\triangle WHP$, angles sum to 180.

Thus $(8q + 17) + (10 + q) + 90 = 180$.

$9q + 117 = 180 \implies 9q = 63 \implies q = 7$. </think>

<answer> 7 </answer>

2. Hard Negatives (y^-)

Reasoning is semantically close (uses geometric properties) but hallucinates constraints.

Neg A (Isosceles Hallucination): <think> Bisector implies $\triangle WHA$ is isosceles. Base angles equal: $8q + 17 = 10 + q \implies 7q = -7 \implies q = -1$. </think> X

Neg B (Summation Error): <think> Sum of given angles is 180 (ignoring right angle). $(8q + 17) + (10 + q) = 180 \implies 9q = 153 \implies q = 17$. </think> X

3. Reflection-Guided Resampling (RGR)

Corrects Neg A using the repair cue.

<think> ... $8q + 17 = 10 + q$...

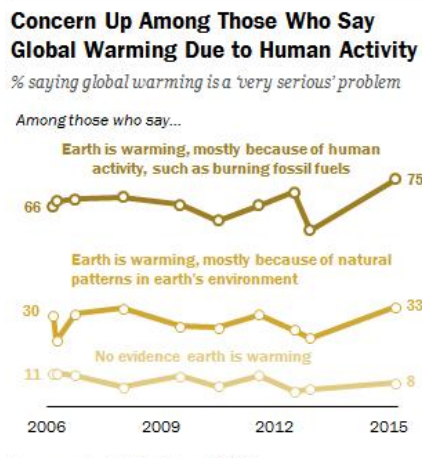
[Correction Trigger]: Wait, perpen. bisector means $\angle WPH = 90^\circ$. I cannot equate the acute angles. They must sum to 90° .

Calculation: $(8q + 17) + (10 + q) = 90 \implies 9q + 27 = 90 \implies 9q = 63 \implies q = 7$. </think>

<answer> 7 </answer> ✓

Figure 13. Analysis of Case 1. The Anchor correctly uses the right-angle property. Hard negatives hallucinate isosceles properties or misapply the sum theorem. RGR successfully recovers from the "equality" hallucination.

Case 2: Multi-Point Data Extraction



Question: What's the product of all the values in 2015?

GT Answer: 19800

1. Anchor (y^+) [Positive]

<think> Locating 2015. Three lines visible.

1. Top (Human activity): 75.
2. Middle (Natural patterns): 33.
3. Bottom (No evidence): 8.

Product: $75 \times 33 \times 8 = 2475 \times 8 = 19800$. </think>

<answer> 19800 </answer>

2. Hard Negatives (y^-)

Correct formula application but fails visual grounding.

Neg A (Visual Omission): <think> Reading 2015. Top is 75. Middle is 33. No other lines clearly visible. Product: $75 \times 33 = 2475$. </think> **X**

Neg B (Data Hallucination): <think> Values are 75, 33, and the bottom looks like 10. Product: $75 \times 33 \times 10 = 24750$. </think> **X**

3. Reflection-Guided Resampling (RGR)

Corrects Neg A (Omission).

<think> ... Product is 2475 ...

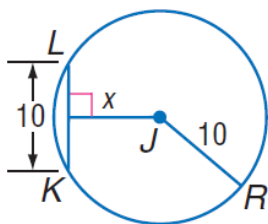
[Correction Trigger]: *Re-checking the chart. I missed the bottom beige line labeled 'No evidence'. The endpoint at 2015 is explicitly 8.*

Revised values: 75, 33, 8. Calculation: $2475 \times 8 = 19800$. </think>

<answer> 19800 </answer> ✓

Figure 14. Analysis of Case 2. Hard negatives often miss the bottom trend line or misread the axis. RGR triggers a visual re-verification step ("Re-checking the chart") to recover the missing data point.

Case 3: Geometry (Circle Properties)



Question: Find x .

GT Answer: $5\sqrt{3}$ (or approx 8.66)

1. Anchor (y^+) [Positive]

Correctly identifies radius and applies Pythagorean theorem.

<think> The radius is $JR = 10$. The segment from center J to any point on the circle is 10, so hypotenuse to L is 10. The perpendicular segment x bisects chord LK . Total chord is 10, so leg is 5.

Pythagoras: $x^2 + 5^2 = 10^2 \implies x^2 + 25 = 100 \implies x^2 = 75$.

$x = \sqrt{75} = 5\sqrt{3}$. </think>

<answer> $5\sqrt{3}$ </answer>

2. Hard Negatives (y^-)

Valid steps (identifying the triangle) but fails on geometric rules.

Neg A (Equilateral Hallucination): <think> Chord is 10, Radius is 10. The triangle formed by the chord and center is equilateral. The line x splits the side. Therefore x is simply half of the side length. $x = 10/2 = 5$. </think> **X**

Neg B (Hypotenuse Confusion): <think> We have a right triangle. The legs are the distance x and the chord length 10. The radius 10 is the hypotenuse. Wait, actually, we form a triangle with sides 10 and 5. $x = \sqrt{10^2 + 5^2} = \sqrt{125} = 5\sqrt{5}$. </think> **X**

3. Reflection-Guided Resampling (RGR)

Corrects Neg A (Equilateral assumption).

<think> ... Triangle is equilateral, so x is half the side, which is 5. ...

[Correction Trigger]: Check the altitude calculation. In an equilateral triangle, the altitude is not half the side; it relates via $\sqrt{3}$.

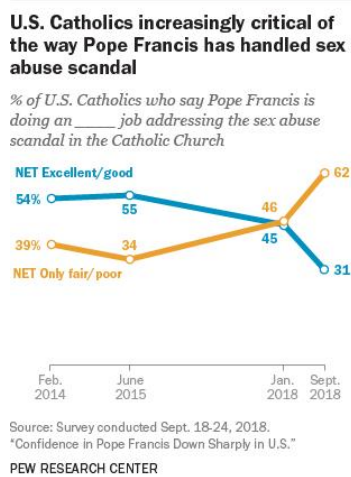
Re-calculating: This is a right triangle with hypotenuse 10 (radius) and base 5 (half-chord).

$x^2 = 100 - 25 = 75$. $x = \sqrt{75} = 5\sqrt{3}$. </think>

<answer> $5\sqrt{3}$ </answer> **✓**

Figure 15. Analysis of Case 3. The model often mistakenly assumes x is a median of length 5 (Neg A) or adds squares instead of subtracting (Neg B). RGR forces a check on the specific right-triangle relationship.

Case 4: Chart Legend Association



Question: What's the blue graph represent?

GT Answer: NET Excellent/good

1. Anchor (y^+) [Positive]

<think> I need to identify the label for the blue line.

1. The blue line starts at 54% and ends at 31%.
2. The text colored in blue/teal directly above the start of the line says "NET Excellent/good".
3. The question asks for the representation.

Result: It represents those saying Pope Francis is doing an excellent or good job.

</think>

<answer> **NET Excellent/good** </answer>

2. Hard Negatives (y^-)

Correct visual attention (looking at lines) but semantic mismatch.

Neg A (Trend Description): <think> The blue line goes down significantly from 54% to 31%. The title says Catholics are "increasingly critical". Therefore, the blue line represents the "Critical" view or the "Sex abuse scandal". </think> **X**

Neg B (Label Swap): <think> There are two lines. The blue one is the lower one at the end (2018). The label nearest to the end of the graph is "NET Only fair/poor" (orange). I will associate the blue line with fair/poor performance. </think> **X**

3. Reflection-Guided Resampling (RGR)

Corrects Neg A (Trend vs Label).

<think> ... The blue line shows the critical trend mentioned in the title. ...

[Correction Trigger]: *Distinguish between the chart title and the specific legend entry. Look for text matching the line's color.*

Correction: The title describes the trend, but the legend defines the data. The text "NET Excellent/good" is colored teal/blue, matching the line. The line represents positive sentiment. </think>

<answer> **NET Excellent/good** </answer> **✓**

Figure 16. Analysis of Case 4. Hard negatives frequently conflate the chart's narrative title with the specific data series (Neg A) or swap legends due to proximity (Neg B). RGR steers the model to verify color-text alignment.